Dissipative stochastic sandpile model on small-world networks: Properties of nondissipative and dissipative avalanches

Himangsu Bhaumik and S. B. Santra*
Department of Physics, Indian Institute of Technology Guwahati, Guwahati-781039, Assam, India
(Received 27 August 2016; published 27 December 2016)

A dissipative stochastic sandpile model is constructed and studied on small-world networks in one and two dimensions with different shortcut densities ϕ, where $\phi = 0$ represents regular lattice and $\phi = 1$ represents random network. The effect of dimension, network topology, and specific dissipation mode (bulk or boundary) on the the steady-state critical properties of nondissipative and dissipative avalanches along with all avalanches are analyzed. Though the distributions of all avalanches and nondissipative avalanches display stochastic scaling at $\phi = 0$ and mean-field scaling at $\phi = 1$, the dissipative avalanches display nontrivial critical properties at $\phi = 0$ and 1 in both one and two dimensions. In the small-world regime ($2^{-12} \leqslant \phi \leqslant 0.1$), the size distributions of different types of avalanches are found to exhibit more than one power-law scaling with different scaling exponents around a crossover toppling size s_c. Stochastic scaling is found to occur for $s < s_c$ and the mean-field scaling is found to occur for $s > s_c$. As different scaling forms are found to coexist in a single probability distribution, a coexistence scaling theory on small world network is developed and numerically verified.

DOI: 10.1103/PhysRevE.94.062138

I. INTRODUCTION

Power-law scaling in many natural phenomena such as earthquakes [1], forest fires [2], biological evolution [3], droplet formation [4], superconducting avalanches [5], etc., are due to the existence of self-organized criticality (SOC) [6] in these systems. SOC refers to the intrinsic tendency of a wide class of slowly driven systems to evolve spontaneously to a nonequilibrium steady state. At the same time, self-organization on complex structures or networks is found to appear very often in nature, for example, the avalanche mode of activity in the neural network of the brain [7], earthquake dynamics on the network of faults in the crust of the Earth [8], rapid rearrangement of the coronal magnetic field network [9], the propagation of information through a network with a malfunctioning router causing the breakdown of the Internet network [10], blackout of the electric power grid [11], and many others. On the other hand, the small-world network (SWN) [12] not only interpolates between the regular lattice and the random network but also preserves both the properties of regular lattice and random network, namely high "clustering-coefficient"(concept of neighborhood) and "small-world effect" (small average shortest distance between any two nodes), respectively. It is always intriguing to study the models of SOC on networks such as SWN.

Sandpile is a prototypical model to study SOC introduced by Bak, Tang, and Wiesenfeld (BTW) [13]. Though BTW on regular lattice gives rise to anomalous (multi) scaling [14,15], it shows a mean-field scaling [16–19] when studied on a random network. A transition from noncritical to critical behavior was reported in a BTW-type sandpile model on SWN in one dimension (1D) [20], whereas a continuous crossover to mean-field behavior was reported for the same model on SWN in 2D [21]. However, recent study of the BTW model on SWN in 2D shows the coexistence of more than one scaling form in the distributions of avalanche properties [19]. On the other hand, stochastic sandpile models (SSM) on regular lattice, which incorporates random distribution of sand grains during avalanche, exhibit a scaling behavior with definite critical exponents that follows finite-size scaling (FSS) and defines a robust universality class called the Manna class [22]. More insight in avalanche size distribution statistics were obtained by classifying the avalanches into dissipative and nondissipative avalanches. The size distribution of dissipative avalanches of BTW sandpile in 2D was found to follow power-law scaling with a definite exponent that does not obey FSS [23]. Later, Dickman and Campelo [24] showed both in one and two dimensions that the dissipative and nondissipative avalanches of SSM on regular lattice obey different FSS behavior with certain logarithmic correction beside the power-law scaling with different exponents. However, there are not many studies that report the critical behavior of SSM and specifically that of the stochastic dissipative avalanches on networks. It is then intriguing to study avalanche size distribution of dissipative and nondissipative avalanches of a stochastic sandpile model on SWN which interpolates regular lattices and random networks and verify whether all such scaling forms would be preserved under bulk dissipation mode.

In this paper, a dissipative stochastic sandpile model (DSSM) is constructed on SWN and studied as a function of shortcut density ϕ in both one and two dimensions. The distribution functions of the steady-state avalanche properties as well as those of dissipative and nondissipative avalanches on regular lattice ($\phi = 0$) and random network ($\phi = 1$) are found to display several interesting nontrivial features. Moreover, in the small-world regime with intermediate ϕ ($\approx 2^{-12}$ to 2^{-3}) [25], the steady-state avalanche properties exhibit coexistence of the SSM scaling and the mean-field scaling in a single distribution depending on the avalanche sizes. A coexistence scaling theory is developed and numerically verified.

II. THE MODEL

SWN is generated both on a 1D linear lattice and on a 2D square lattice by adding shortcuts between any two randomly chosen lattice sites which will be referred to as nodes later.

*santra@iitg.ac.in

The shortcut density ϕ is defined as the number of added shortcuts N_ϕ per existing bond [dL^d bonds are present in a d-dimensional lattice of linear size L with periodic boundary conditions (PBC) and without shortcuts] and is given by $\phi = N_\phi/(dL^d)$. Care has been taken to avoid self-edges of any node and multiedges between any two nodes. To study sandpile dynamics on an SWN, first an SWN is generated for a particular value of ϕ and it is then driven by adding sand grains, one at a time, to randomly chosen nodes. If the height h_i of the sand column at the ith node becomes greater than or equal to the predefined threshold value h_c, which is equal to 2 here, then the ith node topples and the height of the sand column of the ith node will be reduced by h_c. The sand grains toppled are then distributed among two of its randomly selected adjacent nodes which are connected to the toppled node either by shortcuts or by nearest-neighbor bonds. During distribution of the sand grains PBC is applied. Hence, there is no open boundary in the system where dissipation of sand grains could occur. A dissipation factor ϵ_ϕ is then introduced during transport of a sand grain from one node to another to avoid overloading of the system. The toppling rule of the ith critical node in this DSSM on SWN then can be represented as

$$h_i \to h_i - h_c, \quad \text{and} \quad h_j = \begin{cases} h_j + 0 & \text{if } r \leqslant \epsilon_\phi \\ h_j + 1 & \text{otherwise} \end{cases}, \tag{1}$$

where j is two randomly selected nodes of k_i adjacent nodes of the ith node, and r is a random number uniformly distributed over [0,1]. In this distribution rule, an adjacent node may receive both the sand grains. If the toppling of a node causes some of the adjacent nodes to be unstable, subsequent toppling follows on these unstable nodes. The process continues until there is no unstable node present in the system. These toppling activities lead to an avalanche. During an avalanche no sand grain is added to the system.

For a given SWN, ϵ_ϕ is taken as $1/\langle n_\phi \rangle$, where $\langle n_\phi \rangle$ is the average number of steps required for a random walker to reach the lattice boundary (without PBC) starting from an arbitrary lattice site. There exits a characteristic length $\xi \sim \phi^{-1/d}$ where d is the dimensionality of the lattice, below which SWN belongs to the "large world," the regular lattice regime, and beyond which it behaves as "small world," the random network regime [26,27]. The asymptotic behavior of $\langle n_\phi \rangle$ with ϕ and L is given by

$$\langle n_\phi \rangle \sim \begin{cases} L^2, & \phi \to 0 \\ L\phi^{-1/d}, & \phi \to 1 \end{cases} \tag{2}$$

for a d-dimensional SWN. It has diffusive behavior for $\phi \to 0$ and superdiffusive behavior for $\phi \to 1$. The above scaling form is numerically verified in Ref. [19]. The dissipation factor $\epsilon_\phi = 1/\langle n_\phi \rangle$ for a given ϕ is determined using numerically estimated values of $\langle n_\phi \rangle$. A few values of ϵ_ϕ are listed in Table I for 1D and 2D lattices.

TABLE I. Dissipation factor ϵ_ϕ for selected values of ϕ on 1D lattice of $L = 8192$ and 2D square lattice of size $L = 1024$.

	ϵ_ϕ	
ϕ	$d = 1, L = 8192$	$d = 2, L = 1024$
0	8.94×10^{-8}	6.83×10^{-6}
2^{-9}	5.10×10^{-7}	6.34×10^{-5}
2^{-8}	9.72×10^{-7}	9.12×10^{-5}
2^{-7}	1.81×10^{-6}	1.34×10^{-4}
2^{-6}	3.60×10^{-6}	1.99×10^{-4}
2^{-5}	7.10×10^{-6}	2.96×10^{-4}
1	1.27×10^{-4}	2.06×10^{-3}

III. RESULTS AND DISCUSSION

Extensive computer simulations are performed to study the dynamics of DSSM on SWN in 1D and 2D. After a transient period, the system evolves to a steady state which corresponds to equal currents of sand influx and outflux resulting constant average height of the sand columns. Critical properties of DSSM on SWN are characterized studying various avalanche properties in the steady state at different values of ϕ and system size L. The maximum lattice size used for 1D is $L = 8192$ and that for 2D is $L = 1024$. Data are averaged over 32×10^6 avalanches collected on 32 different SWN configurations for a given ϕ and L. The information of an avalanche is kept by storing the number of toppling of every node in an array $S_\phi[i], i = 1, \ldots, L^d$ which was set to zero initially. All geometrical properties of an avalanche such as avalanche size s, avalanche area a, etc., can be estimated in terms of $S_\phi[i]$ as

$$s = \sum_{i=1}^{L^d} S_\phi[i], \quad a = \sum_{i=1}^{L^d} 1 \tag{3}$$

for all $S_\phi[i] \neq 0$.

A. Toppling surface

The values of the toppling number $S_\phi[i]$ of an avalanche at different nodes of SWN define a surface called toppling surface [28] which serves as an important geometrical quantity to visualize an avalanche. The toppling surfaces for typical large avalanches in the steady state, generated on a 1D lattice of size $L = 256$, are presented for $\phi = 0$ and $\phi = 1$, respectively in Figs. 1(a) and 1(b). Toppling surfaces generated on a 2D square lattice of size $L = 256$ are presented in Fig. 1(c) for $\phi = 0$ and for $\phi = 1$ in Fig. 1(d). In both dimensions, the maximum height of the surfaces on regular lattice ($\phi = 0$) is much higher than that on random network ($\phi = 1$). Though the maximum height is much smaller in 1D for $\phi = 1$, all the lattice site toppled more than once, whereas in 2D, the toppling surface on random network consists of mostly singly toppled sites, and only 0.06% of the sites toppled more than once. The toppling surfaces differ considerably on regular lattice and random network in different dimensions.

B. Moment analysis at $\phi = 0$ and 1

The critical steady state of the sandpile model is mostly characterized by power-law scaling of the probability distributions of avalanche size (s) occurring in the steady state. For a given ϕ and L, the probability to have an avalanche of size s is given by $N_{s,\phi}/N_{\text{tot}}$, where $N_{s,\phi}$ is the number of avalanches of

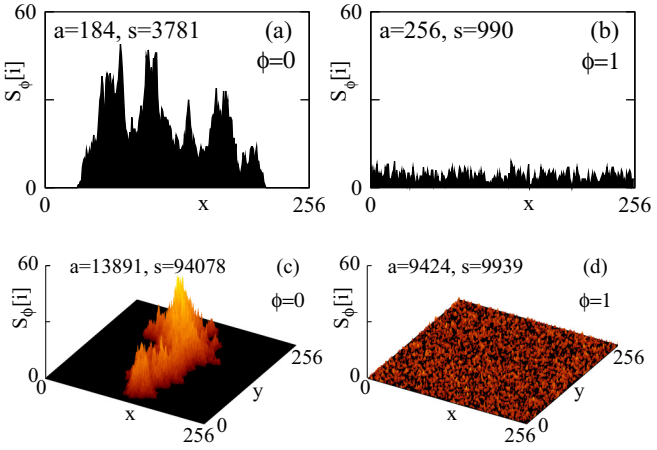

FIG. 1. The toppling surfaces of typical large avalanches of DSSM on SWN are shown. The toppling surface of an avalanche generated on a 1D lattice of size $L = 256$ for $\phi = 0$ is shown in (a) and for $\phi = 1$ is shown in (b). The surface generated on a 2D square lattice of size $L = 256$ for $\phi = 0$ is shown in (c) and for $\phi = 1$ is shown in (d). The size (s) and area (a) of the corresponding avalanches are presented in the respective plots.

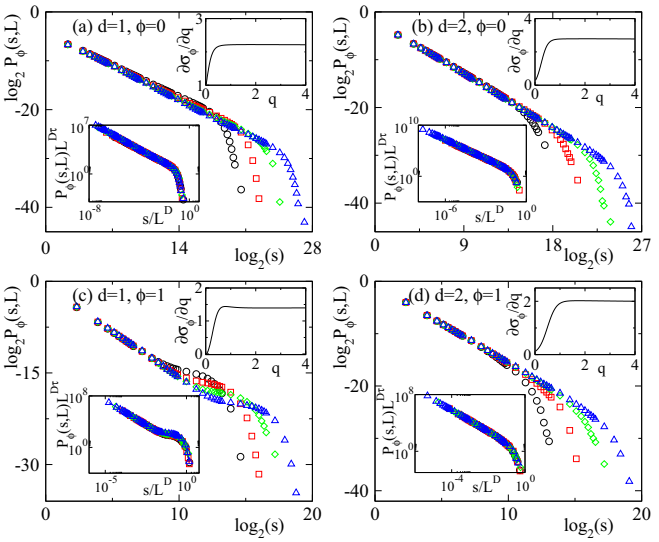

FIG. 2. Plot of $P_\phi(s,L)$ of all the avalanches for $\phi = 0$ (a) for 1D and (b) for 2D. $P_\phi(s,L)$ for $\phi = 1$ are plotted in (c) and (d) for 1D and 2D, respectively. Different curves correspond to different system size L as, for 1D, $L = 2^{10}$ (◯), $L = 2^{11}$ (□), $L = 2^{12}$ (◇), and $L = 2^{13}$ (△), whereas for 2D they are $L = 2^7$ (◯), $L = 2^8$ (□), $L = 2^9$ (◇), and $L = 2^{10}$ (△). Upper inset in each figure shows the plot of $\partial\sigma_\phi(q)/\partial q$ against q, whereas the lower inset shows the corresponding FSS data collapse.

size s of the total number of avalanches $N_{\rm tot}$ generated at the steady state. The distribution of s follows a power-law scaling with a well-defined exponent τ and obeys FSS [14]. The FSS form of the probability distribution of s in DSSM is given by

$$P_\phi(s,L) = s^{-\tau} f_\phi\left[\frac{s}{L^D}\right], \tag{4}$$

where f_ϕ is a ϕ-dependent scaling function and D is the capacity dimension. Very often the power-law scaling is found to sustain over a short range of avalanche sizes and hinders precise extraction of the exponent τ from the slope of the plot of $P_\phi(s,L)$ against s in double logarithmic scale. A more reliable estimate of the exponent can be made employing moment analysis [15,29]. For a given ϕ, the qth moment of s is defined as

$$\langle s^q(L)\rangle_\phi = \int_0^\infty s^q P_\phi(s,L) ds \sim L^{\sigma_\phi(q)}, \tag{5}$$

where

$$\sigma_\phi(q) = D(q - \tau + 1) \tag{6}$$

is the moment scaling function for $q > \tau - 1$ [for $q < \tau - 1$, $\sigma_\phi(q) = 0$]. Values of $\sigma_\phi(q)$ are estimated from the slope of the plots of $\langle s^q(L)\rangle_\phi$ versus L in double logarithmic scale for 400 equidistant values of q between 0 and 4. The value of D can be measured from the saturated value of $\partial\sigma_\phi(q)/\partial q$ in the large-q limit. The derivative $\partial\sigma_\phi(q)/\partial q$ is determined numerically by the finite-difference method. Once D is known the exponent τ can be estimated from Eq. (6) using the value of $\sigma_\phi(1)$.

1. All avalanches

$P_\phi(s,L)$ of all the avalanches for various values of L are presented in Fig. 2 for 1D and 2D for $\phi = 0$ and 1. Reasonable power-law scaling is observed for these extreme values of ϕ in both the dimensions. The flat tail in $P_\phi(s,L)$ for $\phi = 1$ in 1D is due to large dissipative avalanches, which will be discussed later separately. Employing moment analysis, values of D and τ are estimated for all four situations. For $\phi = 0$, estimates of D are found to be 2.21 ± 0.02 and 2.76 ± 0.02 for 1D and 2D, respectively. Since for $\phi = 0$, $\sigma_\phi(1) \approx 2$ in both the dimensions, the values of τ estimated from Eq. (6) are 1.09 ± 0.02 in 1D and 1.28 ± 0.01 in 2D. As expected, the exponents are found very close to the reported values for SSM on regular lattice in respective dimensions, for instance, $\tau = 1.112 \pm 0.006$, $D = 2.253 \pm 0.014$ in 1D and $\tau = 1.273 \pm 0.002$, $D = 2.750 \pm 0.006$ in 2D [30], whereas for $\phi = 1$, the values of D are found to be 1.39 ± 0.02 and ≈ 2 in 1D and 2D, respectively. In 2D, the avalanches on random network ($\phi = 1$) consist mostly of single toppled nodes, and hence $D \approx 2$ is expected, whereas the value of $D > 1$ in 1D suggests that the avalanches consist of multiple toppled nodes. In both the dimensions, the value of τ for $\phi = 1$ is ≈ 1.50, the mean-field value as obtained in branching processes [16–18]. The values of the exponents are listed in Table II. The FSS form of $P_\phi(s,L)$ is verified by plotting the scaled distribution $P_\phi(s,L)L^{D\tau}$ against the scaled variable s/L^D in the respective lower inset of Fig. 2 using the respective values of the critical exponents obtained.

2. Nondissipative and dissipative avalanches

Avalanches are now classified into nondissipative and dissipative avalanches. During the evolution, a dissipative avalanche must dissipate at least a sand grain once, whereas no sand grain be dissipated in a nondissipative avalanche. The avalanche size distribution $P_\phi(s,L)$ can be written in terms of $P_{\phi,\rm nd}(s,L)$ and $P_{\phi,d}(s,L)$, the distributions of nondissipative

TABLE II. Best estimated values of D and τ for DSSM in 1D and 2D at $\phi = 0$ and at $\phi = 1$ for nondissipative avalanches, dissipative avalanches, and all avalanches. As the values of D is estimated from $\partial\sigma_\phi(q)/\partial q$ the error in determination of D is $2\Delta q$, i.e., ± 0.020. The number in the parentheses is the uncertainty of last digit of the value τ determined from the scaling relations.

		Nondissipative	Dissipative	all
1D	$\phi = 0$	$D_{\rm nd} = 2.009$ $\tau_{\rm nd} = 1.11(2)$	$D_d = 2.214$ $\tau_d = 0.14(1)$	$D = 2.215$ $\tau = 1.09(2)$
	$\phi = 1$	$D_{\rm nd} = 1.022$ $\tau_{\rm nd} = 1.52(2)$	$D_d = 1.402$ $\tau_d = 0.54(2)$	$D = 1.395$ $\tau = 1.50(1)$
2D	$\phi = 0$	$D_{\rm nd} = 2.004$ $\tau_{\rm nd} = 1.29(1)$	$D_d = 2.791$ $\tau_d = 0.40(2)$	$D = 2.764$ $\tau = 1.28(1)$
	$\phi = 1$	$D_{\rm nd} = 1.013$ $\tau_{\rm nd} = 1.54(5)$	$D_d = 2.023$ $\tau_d = 1.45(3)$	$D = 2.008$ $\tau = 1.51(2)$

and dissipative avalanches, as

$$P_\phi(s,L) = P_{\phi,\rm nd}(s,L) + P_{\phi,d}(s,L) \tag{7}$$

with

$$P_{\phi,\rm nd}(s,L) = \frac{n_{s,\rm nd}}{N_{\rm tot}} \quad \text{and} \quad P_{\phi,d}(s,L) = \frac{n_{s,d}}{N_{\rm tot}}, \tag{8}$$

where $n_{s,\rm nd}$ and $n_{s,d}$ are number of nondissipative and dissipative avalanches of size s of a total of $N_{\rm tot}$ avalanches. First, the analysis of nondissipative avalanches is given and then that of dissipative avalanches is presented.

The FSS form of the distribution $P_{\phi,\rm nd}(s,L)$ is assumed to be

$$P_{\phi,\rm nd}(s,L) = s^{-\tau_{\rm nd}} f_{\phi,\rm nd}\left[\frac{s}{L^{D_{\rm nd}}}\right], \tag{9}$$

where $f_{\phi,\rm nd}$ is a scaling function and $\tau_{\rm nd}$ and $D_{\rm nd}$ are the respective exponents. $P_{\phi,\rm nd}(s,L)$ for $\phi = 0$ and 1 are plotted in Fig. 3 for several values of L for both 1D and 2D. Performing moment analysis, the values of $D_{\rm nd}$ are found as $D_{\rm nd} \approx 2$ for $\phi = 0$ and $D_{\rm nd} \approx 1$ for $\phi = 1$ in both 1D and 2D. It could be recalled here that the dissipation factor is chosen from the inverse of $\langle n_\phi \rangle$. On an average the avalanche of size $s > \langle n_\phi \rangle/2$ must dissipate at least one sand grain (the factor 2 is for one toppling consists two sand transfer). Since $\langle n_\phi \rangle \sim L^2$ as $\phi \to 0$ due to diffusive behavior of random walker on regular lattice and $\langle n_\phi \rangle \sim L$ as $\phi \to 1$ for superdiffusive behaviour of random walker on random network [19], the cutoff of $P_{\phi,\rm nd}(s,L)$ must scale with L in the same way as $\langle n_\phi \rangle$ scales with L. Knowing the values of $D_{\rm nd}$ and $\sigma_{\phi,\rm nd}(1)$, the values of $\tau_{\rm nd}$ are estimated. The values of $\sigma_{\phi,\rm nd}(1)$ are found as 1.78 for $\phi = 0$ and 0.48 for $\phi = 1$ in 1D. Accordingly, $\tau_{\rm nd} = 1.11(2)$ for $\phi = 0$ and $\tau_{\rm nd} = 1.52(2)$ for $\phi = 1$ in 1D. The power-law scaling of $P_{\phi,\rm nd}(s,L)$ is found similar to that of $P_\phi(s,L)$ as the values of τ and $\tau_{\rm nd}$ are found more or less same for both the distributions for $\phi = 0$ and 1, whereas, in 2D, the values of the exponents are found as $\tau_{\rm nd} = 1.29 \pm 0.01$ for $\phi = 0$ [since $\sigma_{\phi,\rm nd}(1) = 1.4$] and $\tau_{\rm nd} = 1.54 \pm 0.05$ for $\phi = 1$ as $\sigma_{\phi,\rm nd}(1) = 0.5$. On regular lattice it is the SSM result, whereas on random network it is the mean-field result. The values of $D_{\rm nd}$ and $\tau_{\rm nd}$ for nondissipative avalanches are listed in Table II. Using the values of $\tau_{\rm nd}$ and $D_{\rm nd}$, a reasonable data collapse is obtained for $P_{\phi,\rm nd}(s,L)$ as shown in the lower insets of Fig. 3.

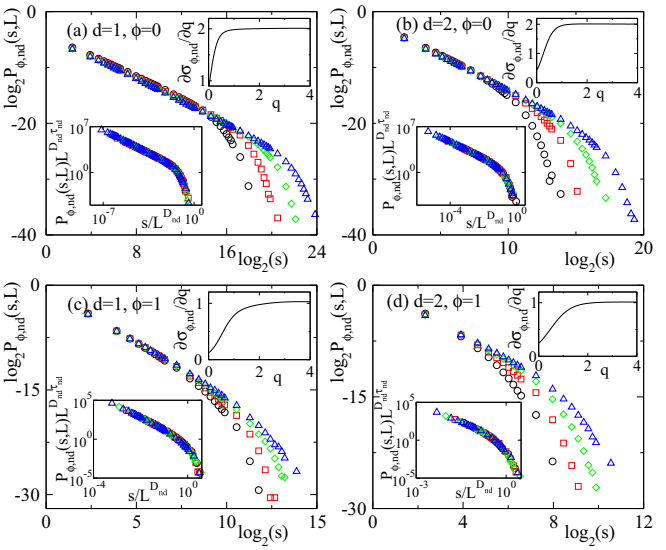

FIG. 3. Plot of $P_{\phi,\rm nd}(s,L)$ for different L (with same symbol as in Fig. 2) for $\phi = 0$ in (a) for 1D and in (b) for 2D. For $\phi = 1$ the same has been plotted in (c) and (d) for 1D and 2D, respectively. Insets in each figure are same as that of Fig. 2 but for nondissipative avalanches.

The size distribution of dissipative avalanches $P_{\phi,d}(s,L)$ for several values of L are presented in Fig. 4 for $\phi = 0$ and 1 in both the dimensions. Interestingly, the distributions $P_{\phi,d}(s,L)$ are very different in nature than the corresponding $P_{\phi,\rm nd}(s,L)$. Preliminary estimate of the size distribution exponent τ_d by linear least-squares fit to the data points in double-logarithmic scale reveals that $\tau_d < 1$ except for $\phi = 1$ in 2D. Following Christensen and coworkers [31], a new scaling form of

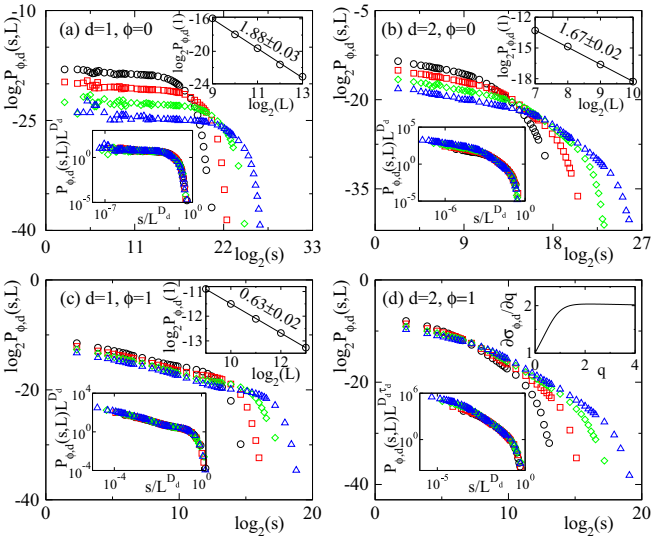

FIG. 4. Plot of $P_{\phi,d}(s,L)$ for various L (with same symbol as in Fig. 2) for $\phi = 0$ in (a) for 1D and in (b) for 2D. For $\phi = 1$ the same has been plotted in (c) and (d) for 1D and 2D, respectively. Upper insets: (a)–(c) show the plot of $P_{\phi,d}(1,L)$ against L, and (d) shows variation of $\partial\sigma_{\phi,d}(q)/\partial q$ against q. Lower insets shows the corresponding FSS data collapse (see text).

$P_{\phi,d}(s,L)$ is proposed as

$$P_{\phi,d}(s,L) = s^{-\tau_d} L^{D_d(\tau_d-1)} f_{\phi,d}\left[\frac{s}{L^{D_d}}\right], \tag{10}$$

where $f_{\phi,d}$ is a new scaling function and τ_d and D_d are exponents for dissipative avalanches. The moment of such a distribution is obtained as $\langle s^q(L)\rangle_{\phi,d} \sim L^{\sigma_{\phi,d}(q)}$, where $\sigma_{\phi,d}(q) = qD_d$. Noticeably, the moment exponent $\sigma_{\phi,d}(q)$ becomes independent of the size distribution exponent τ_d. Performing moment analysis for both 1D and 2D, the values of D_d for dissipative avalanches are found close to that of the all avalanches as presented in Table II. In the limit $s/L^{D_d} \to 0$, the scaling function $f_{\phi,d}[s/L^{D_d}]$ becomes a constant and the distribution is given by $P_{\phi,d}(s,L) \approx s^{-\tau_d} L^{D_d(\tau_d-1)}$. Consequently, $P_{\phi,d}(1,L) \sim L^{D_d(\tau_d-1)}$ for $s = 1$. The exponent τ_d is then estimated from the slope of the plot of $P_{\phi,d}(1,L)$ vs L in double logarithmic scale as presented in the upper insets of Figs. 4(a)–4(c). The values of τ_d are estimated as 0.14 ± 0.01 for $\phi = 0$ and 0.54 ± 0.01 for $\phi = 1$ in 1D. It is interesting to note that such a flat distribution (i.e., $\tau_d \to 0$ for $\phi = 0$ in 1D) is also reported by Amaral and Lauritsen [32] for the dissipative avalanches of a 1D rice pile model. In contrast to the present observation, Dickman and Campelo [24] found a power-law scaling of $P_d(s,L)$ with exponent $\tau_d = 0.637$ for SSM with boundary dissipation on 1D regular lattice. In 2D, the exponent τ_d is obtained here as 0.40 ± 0.02 for $\phi = 0$, whereas Dickman and Campelo [24] reported $\tau_d = 0.98$ for SSM on a 2D regular lattice with boundary dissipation. Thus the scaling behavior of dissipative avalanches of DSSM differs substantially from that of dissipative avalanches of SSM with boundary dissipation in both the dimensions at $\phi = 0$. Such difference in the scaling behavior for dissipative avalanches with different modes of dissipation is probably due to different topological properties of network in the bulk and at the boundary because the degree of a node at the boundary differs from that of a node in the bulk. Moreover, it should be noted that for the model of boundary dissipation, Dickman and Campelo introduced a logarithmic correction in the distribution of dissipative avalanches and the distribution was given by

$$P_{dc}(s,L) = s^{-\tau_d} [\ln(s)]^{\eta} f_{dc}\left[\frac{s}{L^{D}}\right], \tag{11}$$

where η is an another exponent. In order to verify the presence or absence of such a correction to scaling in the present model with bulk dissipation, the scaling function $f_{\phi,d}$ given in Eq. (10) for $\phi = 0$ is plotted in Figs. 5(a) and 5(b) for 1D and 2D, respectively. For comparison, the scaling function f_{dc} of the model with boundary dissipation given in Eq. (11) is also plotted in the respective plots. It can be seen that without any correction, the scaling function $f_{\phi,d}$ is reasonably constant over a wide range of s in double logarithmic scale in the case of bulk dissipation, whereas it requires a correction to scaling, $[\ln(s)]^{\eta}$, in the case of boundary dissipation for $d = 2$ ($\eta = 0.5$), as observed by Dickman and Campelo [24]. Hence the scaling forms considered here for the model with bulk dissipation are not subject to any logarithmic correction. However, the scaling behavior of all avalanches are found to be same for both the models as reported in Ref. [33]. This is because the leading singularity is provided by nondissipative avalanches. In order to verify the form of the scaling function given the Eq. (10), data collapse has been performed by plotting $P_{\phi,d}(s,L)L^{D_d}$ against s/L^{D_d} for different values of L. Reasonable data collapse for different $P_{\phi,d}(s,L)$ are obtained as shown in the respective lower insets of Fig. 4. For $\phi = 1$ in 2D, the FSS form of the distribution $P_{\phi,d}(s,L)$ is expected to follow the usual distribution as given in Eq. (4). From the plot of $\partial\sigma_{\phi,d}(q)/\partial q$ vs q as given in upper inset of Fig. 4(d), D_d is found to be 2.023 ± 0.020, again close to the value of all avalanches. The value of τ_d is estimated from Eq. (6) as 1.45 ± 0.03, which is a little less than mean-field result as obtained for the all avalanches. However, taking $\tau_d = 3/2$ and $D_d = 2.023$ the best data collapse is obtained, given in the lower inset of Fig. 4(d), which confirms the respective form of the scaling function. It should be noted here that the value of D_d for dissipative avalanches are very close to the value of D of the all avalanches for both the extreme values of ϕ in both the dimensions because the large avalanches which are responsible for cutoff of the distribution of all avalanches are mostly dissipative, and in the moment analysis the leading contribution comes from those large dissipative avalanches.

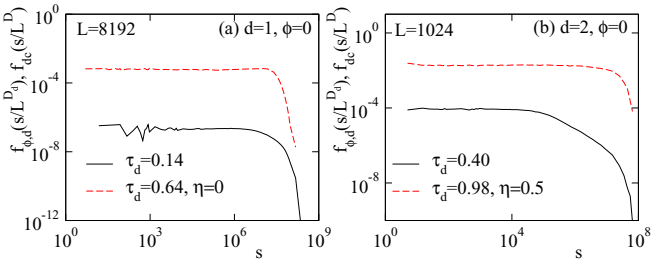

FIG. 5. Plot of $f_{\phi,d}(= P_{\phi,d}(s)s^{\tau_d})$ (in solid black line) and $f_{dc}(= P_{\phi,d}(s)s^{\tau_d}[\ln(s)]^{-\eta})$ (in dashed red line) against s for 1D, $L = 8192$, in (a) and for 2D, $L = 1024$, in (b). The values of the τ_d and η for f_{dc} are taken from Ref. [24]. Since the plots are for a given L, the L dependency of the argument is dropped.

C. Small-world regime

1. *Scaling properties*

Since SWN preserves both the characteristics of regular lattice and random network, it is important to study the critical properties of the avalanche size distribution in the SWN regime, $2^{-12} < \phi < 0.1$. The size distribution $P_\phi(s)$ of all the avalanches are plotted in Fig. 6(a) for 1D and in Fig. 6(b) for 2D. In Figs. 6(c) and 6(d), $P_{\phi,d}(s)$ are plotted for 1D and 2D, respectively. For 1D and 2D, the values of ϕ used are 2^{-6} and 2^{-8}, respectively, for both the distributions. Interestingly, both the distributions $P_\phi(s)$ and $P_{\phi,d}(s)$ exhibit their respective scaling forms on regular lattice ($\phi = 0$) and random network ($\phi = 1$) in the same distribution. The straight lines with respective slopes in these plots are guides to the eye. The crossover from one scaling form to other occurs at their respective crossover avalanche size s_c for $P_\phi(s)$ and $P_{\phi,d}(s)$. For $s < s_c$, the avalanches are small, compact, and mostly confined on a regular lattice, whereas for $s > s_c$ they are large, sparse, and mostly exposed to random network. Since $P_{\phi,\mathrm{nd}}(s)$ and $P_\phi(s)$ have similar scaling behavior, $P_{\phi,\mathrm{nd}}(s)$ display a

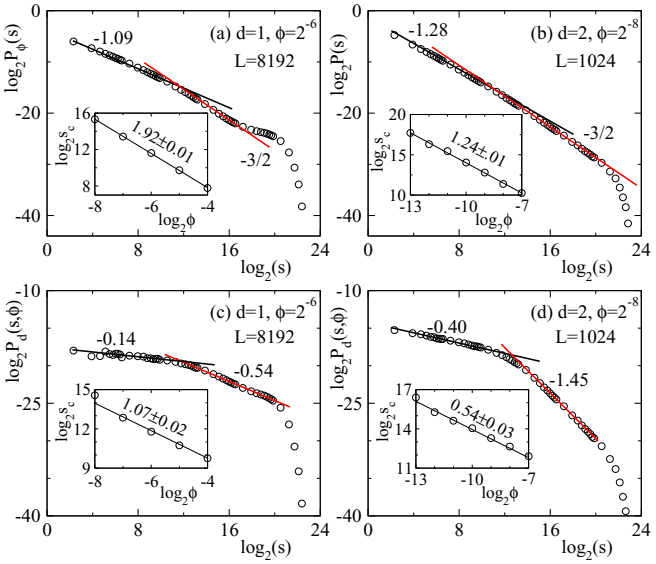

FIG. 6. Plot of $P_\phi(s)$ against s in (a) for 1D with $\phi = 2^{-6}$ for $L = 8192$ and in (b) for 2D with 2^{-8} for $L = 1024$. The corresponding $P_d(s,\phi)$ is shown in (c) for 1D and in (d) for 2D. The solid lines with the required slope through the data points are guide to eye. The variation of s_c with ϕ is shown in the respective inset. The error in estimation of s_c is of the order of the symbol size.

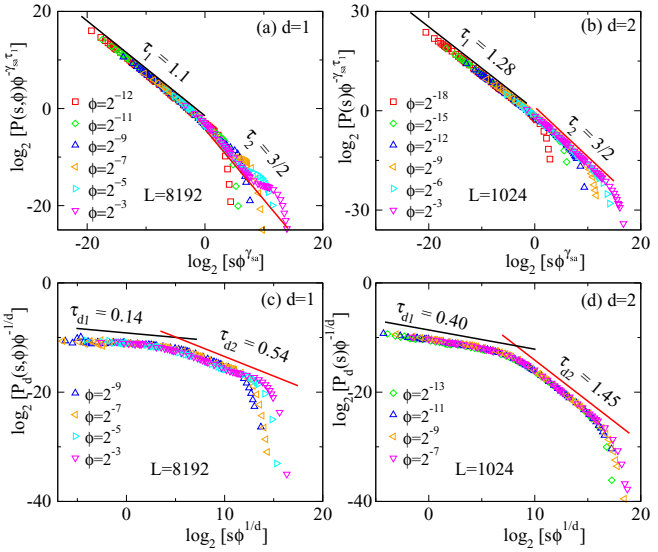

FIG. 7. Scaled probability distribution (for all avalanches) against scaled variable is plotted for selected values of ϕ in (a) for 1D with $L = 8192$ and in (b) for 2D with $L = 1024$ to verify the scaling forms given in Eq. (14). The same has been verified for dissipative avalanches in (c) for 1D and in (d) for 2D.

similar crossover scaling as that of $P_\phi(s)$. The coexistence of more than one scaling form in the same distribution of avalanche properties for different sandpile models has been already reported in the literature [19,20,34]. The crossover scaling is found to occur for a wide range of ϕ within the SWN regime for both $P_\phi(s)$ and $P_{\phi,d}(s)$. As one expects the scaling form of regular lattice as $\phi \to 0$ and that of random network as $\phi \to 1$, the value of s_c is found to depend on ϕ for both the distributions. The dependence of s_c on ϕ is assumed as

$$s_c \sim \phi^{-\alpha}, \tag{12}$$

where α is an exponent. The value of α for all avalanches can be obtained by simple arguments. From the conditional expectation of avalanche size for a fixed avalanche area, one expects $s_c \sim a_c^{\gamma_{sa}} \approx \xi^{d\gamma_{sa}}$, where a_c is the average avalanche area for the avalanches of size s_c, γ_{sa} is an exponent [16], and ξ is the crossover length scale below which SWN behaves as regular lattice [26,27]. As $\xi \sim \phi^{-1/d}$, one obtains $s_c \sim \phi^{-\gamma_{sa}}$ and has $\alpha = \gamma_{sa}$. However, a dissipative avalanche occurs only after a required number of toppling equivalently $\langle n_\phi \rangle$. As $\langle n_\phi \rangle \sim \phi^{-1/d}$ in the large-ϕ limit corresponding to random network, one expects $s_c \sim \phi^{-1/d}$ with $\alpha = 1/d$. For a given ϕ the value of s_c is estimated from the intersection point of the straight lines with required slope in the respective regions. The estimated values of s_c is then plotted against ϕ in double logarithmic scale in the respective insets of Fig. 6. It can be seen that in all cases s_c shows a reasonable power-law scaling with ϕ. By linear least-squares fit through the data points the values of α for all avalanches are found to be 1.92 ± 0.01 for 1D and 1.24 ± 0.01 for 2D which are very close to the γ_{sa} values at $\phi = 0$ in both dimensions [35,36]. On the other hand, for dissipative avalanches it is found that $\alpha = 1.07 \pm 0.02$ for 1D and $\alpha = 0.54 \pm 0.03$ for 2D, again close the inverse of respective dimensions.

2. *Coexistence scaling*

Since FSS forms of $P_\phi(s,L)$ and $P_{\phi,d}(s,L)$ are found to be satisfied both on regular lattice and on random network, they should also be satisfied on SWN. Instead of FSS form, the ϕ dependence of these distributions are then verified on SWN for a fixed L. A generalized scaling form for $P(s,\phi)$ for the all avalanches on SWN is proposed as

$$P(s,\phi) = \begin{cases} s^{-\tau_1} \mathsf{f}\left(\frac{s}{s_c(\phi)}\right) & \text{for } s \leqslant s_c \\ s^{-\tau_2} \mathsf{g}\left(\frac{s}{s_c(\phi)}\right) & \text{for } s \geqslant s_c \end{cases}, \tag{13}$$

where f and g are the respective scaling functions and τ_1, τ_2 are the corresponding critical exponents in the $s < s_c$ and $s > s_c$ regions, respectively. At $s = s_c$ for a given ϕ, the limiting values of $P(s,\phi)$ from both the regions must be the same. As $s_c \sim \phi^{-\alpha}$, then one should have $\phi^{\tau_1\alpha}\mathsf{f}(1) = \phi^{\tau_2\alpha}\mathsf{g}(1)$. Hence, the ϕ-independent scaled distribution can be obtained as

$$P(s,\phi)\phi^{-\alpha\tau_1} = \begin{cases} (s\phi^\alpha)^{-\tau_1}\mathsf{f}(s\phi^\alpha) & \text{for } s \leqslant s_c \\ (s\phi^\alpha)^{-\tau_2}\mathsf{f}(s\phi^\alpha) & \text{for } s \geqslant s_c \end{cases}, \tag{14}$$

in terms of a single scaling function f [19]. Such a scaling form is also found to exist in the dynamic scaling of roughness of fractured surfaces [37]. To verify the scaling forms given in Eq. (14), the scaled probabilities for all avalanches are plotted against the scaled variable in Figs. 7(a) and 7(b) for 1D and 2D, respectively, taking $\alpha = \gamma_{sa}$. It can be seen that a good data collapse is obtained using $\gamma_{sa} = 2$, $\tau_1 = 1.1$ for 1D and using $\gamma_{sa} = 1.26$, $\tau_2 = 1.28$ for 2D. The straight lines with required slopes in the respective regions are guide to eye. It confirms the validity of the proposed scaling function form given in Eq. (13). Similarly, a generalized size distribution

function can be written for dissipative avalanches around its crossover size s_c taking $\alpha = 1/d$. The scaled probabilities for $P_d(s,\phi)\phi^{-1/d}$ for dissipative avalanches are plotted against the scaled variable $s\phi^{1/d}$ in Figs. 7(c) and 7(d) for 1D and 2D respectively. Reasonable data collapse is obtained as expected. It is then important to notice that if a dynamical model like sandpile is studied on SWN, multiple scaling forms of an event size will coexist in the distribution of the same.

IV. SUMMARY AND CONCLUSION

A dissipative stochastic sandpile model is developed and its critical properties are studied on SWNs both in 1D and 2D for a wide range of shortcut density ϕ. The nondissipative avalanches display usual stochastic scaling of SSM on regular lattice ($\phi = 0$) and mean-field scaling on random network ($\phi = 1$) as that of all avalanches. However, the dissipative avalanches represent a number of novel scaling properties on regular lattice as well as on random network in both 1D and 2D. The scaling behavior of these avalanches on regular lattice is found to differ considerably from Dickman-Campelo scaling as observed with the open boundary in both dimensions. The bulk dissipation is found to have a nontrivial effect on dissipative avalanches over the boundary dissipation. No logarithmic correction to scaling is found to occur as it was required for these avalanches on regular lattice with boundary dissipation. A set of new scaling exponents are found to describe the scaling of dissipative avalanches on regular lattice and random network. On SWN, in the intermediate range of ϕ, the model exhibits coexistence of more than one scaling form in both 1D and 2D around a crossover size $s_c(\phi)$. For nondissipative and dissipative avalanches, however, the crossover size s_c scales with ϕ with two different exponents. The small, compact avalanches of size $s < s_c$ mostly confined on regular lattice are found to obey the usual SSM scaling, whereas the large, sparse avalanches of size $s > s_c$ exposed to random network are found to obey mean-field scaling. A coexistence scaling form of the avalanche size distribution function around s_c is proposed and numerically verified. Therefore, SWN can be considered as a segregator of several scaling forms that appear in the event size distribution in a dynamical system.

ACKNOWLEDGMENTS

This work was partially supported by the Department of Science and Technology, Ministry of Science and Technology, Government of India, through Project No. SR/S2/CMP-61/2008. Availability of the computational facility "Newton HPC" under the FIST project of the Department of Physics, IIT Guwahati funded by the Department of Science and Technology, Ministry of Science and Technology, Government of India, is gratefully acknowledged.

[1] K. Chen, P. Bak, and S. P. Obukhov, Phys. Rev. A **43**, 625 (1991).
[2] B. Drossel and F. Schwabl, Phys. Rev. Lett. **69**, 1629 (1992); B. Drossel, S. Clar, and F. Schwabl, *ibid.* **71**, 3739 (1993).
[3] P. Bak and K. Sneppen, Phys. Rev. Lett. **71**, 4083 (1993).
[4] B. Plourde, F. Nori, and M. Bretz, Phys. Rev. Lett. **71**, 2749 (1993).
[5] S. Field, J. Witt, F. Nori, and X. Ling, Phys. Rev. Lett. **74**, 1206 (1995).
[6] P. Bak, *How Nature Works: The Science of Self-Organized Criticality* (Copernicus, New York, 1996); H. J. Jensen, *Self-Organized Criticality* (Cambridge University Press, Cambridge, 1998); K. Christensen and N. R. Moloney, *Complexity and Criticality* (Imperial College Press, London, 2005); G. Pruessner, *Self- Organized Criticality: Theory, Models and Characterization* (Cambridge University Press, Cambridge, 2012).
[7] L. de Arcangelis, C. Perrone-Capano, and H. J. Herrmann, Phys. Rev. Lett. **96**, 028107 (2006); J. Hesse and T. Gross, Front. Syst. Neurosci. **8**, 166 (2014).
[8] S. Lise and M. Paczuski, Phys. Rev. Lett. **88**, 228301 (2002).
[9] D. Hughes, M. Paczuski, R. O. Dendy, P. Helander, and K. G. McClements, Phys. Rev. Lett. **90**, 131101 (2003).
[10] A. E. Motter and Y.-C. Lai, Phys. Rev. E **66**, 065102 (2002).
[11] B. Carreras, D. Newman, I. Dobson, and A. Poole, IEEE Trans. Circ. Syst. I **51**, 1733 (2004).
[12] D. Watts and S. Strogatz, Nature **393**, 440 (1998).
[13] P. Bak, C. Tang, and K. Wiesenfeld, Phys. Rev. Lett. **59**, 381 (1987); Phys. Rev. A **38**, 364 (1988).
[14] M. DeMenech, A. L. Stella, and C. Tebaldi, Phys. Rev. E **58**, R2677 (1998); C. Tebaldi, M. DeMenech, and A. L. Stella, Phys. Rev. Lett. **83**, 3952 (1999).
[15] S. Lübeck, Phys. Rev. E **61**, 204 (2000).
[16] K. Christensen and Z. Olami, Phys. Rev. E **48**, 3361 (1993).
[17] E. Bonabeau, J. Phys. Soc. Jpn. **64**, 327 (1995).
[18] K.-I. Goh, D.-S. Lee, B. Kahng, and D. Kim, Phys. Rev. Lett. **91**, 148701 (2003).
[19] H. Bhaumik and S. B. Santra, Phys. Rev. E **88**, 062817 (2013).
[20] J. Lahtinen, J. Kertész, and K. Kaski, Physica A **349**, 535 (2005).
[21] L. de Arcangelis and H. Herrmann, Physica A **308**, 545 (2002).
[22] S. S. Manna, J. Phys. A **24**, L363 (1991); D. Dhar, Physica A **263**, 4 (1999), and references therein .
[23] B. Drossel, Phys. Rev. E **61**, R2168 (2000).
[24] R. Dickman and J. M. M. Campelo, Phys. Rev. E **67**, 066111 (2003).
[25] M. E. J. Newman, A.-L. Barabasi, and D. J. Watts, The Structure and Dynamics of Networks, *Princeton Studies in Complexity* (Princeton University Press, Princeton, NJ, 2006).
[26] M. E. J. Newman and D. J. Watts, Phys. Rev. E **60**, 7332 (1999); Phys. Lett. A **263**, 341 (1999).
[27] M. A. de Mendes, C. F. Moukarzel, and T. J. P. Penna, Europhys. Lett. **50**, 574 (2000).
[28] J. A. Ahmed and S. B. Santra, Europhys. Lett. **90**, 50006 (2010).
[29] R. Karmakar, S. S. Manna, and A. L. Stella, Phys. Rev. Lett. **94**, 088002 (2005).
[30] H. Huynh, G. Pruessner, and L. Chew, J. Stat. Mech (2011) P09024. H. N. Huynh and G. Pruessner, Phys. Rev. E **85**, 061133 (2012).
[31] N. Farid and K. Christensen, New J. Phys. **8**, 212 (2006); K. Christensen, N. Farid, G. Pruessner, and M. Stapleton, Eur. Phys. J. B **62**, 331 (2008).

[32] Luís A. Nunes Amaral and K. B. Lauritsen, Phys. Rev. E **54**, R4512(R) (1996).

[33] O. Malcai, Y. Shilo, and O. Biham, Phys. Rev. E **73**, 056125 (2006).

[34] M. Hoore and S. Moghimi-Araghi, J. Phys. A: Math. Theor. **46**, 195001 (2013); S. Moghimi-Araghi and M. Sebtosheikh, Phys. Rev. E **92**, 022116 (2015); S. A. Moosavi and A. Montakhab, *ibid.* **92**, 052804 (2015).

[35] H. Nakanishi and K. Sneppen, Phys. Rev. E **55**, 4012 (1997).

[36] A. Ben-Hur and O. Biham, Phys. Rev. E **53**, R1317 (1996); S. B. Santra, S. Ranjita Chanu, and D. Deb, *ibid.* **75**, 041122 (2007).

[37] J. M. López and J. Schmittbuhl, Phys. Rev. E **57**, 6405 (1998); S. Morel, J. Schmittbuhl, J. M. López, and G. Valentin, *ibid.* **58**, 6999 (1998).